Closed-Loop Control of Complex Networks: A Trade-Off between Time and Energy

Yong-Zheng Sun,[1,2] Si-Yang Leng,[1,3,4] Ying-Cheng Lai,[5] Celso Grebogi,[6] and Wei Lin[1,3,*]

[1]*Center for Computational Systems Biology of ISTBI, Fudan University, Shanghai 200433, China*
[2]*School of Mathematics, China University of Mining and Technology, Xuzhou 221116, China*
[3]*School of Mathematical Sciences and LMNS, Fudan University, Shanghai 200433, China*
[4]*Collaborative Research Center for Innovative Mathematical Modelling, Institute of Industrial Science,*
The University of Tokyo, Tokyo 153-8505, Japan
[5]*School of Electrical, Computer, and Energy Engineering, Arizona State University, Tempe, Arizona 85287-5706, USA*
[6]*Institute for Complex Systems and Mathematical Biology, University of Aberdeen, Aberdeen AB24 3UE, United Kingdom*

Controlling complex nonlinear networks is largely an unsolved problem at the present. Existing works focus either on open-loop control strategies and their energy consumptions or on closed-loop control schemes with an infinite-time duration. We articulate a finite-time, closed-loop controller with an eye toward the physical and mathematical underpinnings of the trade-off between the control time and energy as well as their dependence on the network parameters and structure. The closed-loop controller is tested on a large number of real systems including stem cell differentiation, food webs, random ecosystems, and spiking neuronal networks. Our results represent a step forward in developing a rigorous and general framework to control nonlinear dynamical networks with a complex topology.

Recent years have witnessed a growth of interest in controlling complex networks. A vast majority of the existing works in this area dealt with the controllability and control of linear dynamical networks [1–27]. Controlling complex networks with nonlinear dynamics has been limited to brute force strategies such as local pinning [28–31] or to specific systems exhibiting a simple kind of multistability [32–36]. Most existing methods of controlling nonlinear networks were of the open-loop type; i.e., one selects a suitable subset of nodes and applies *predefined* control signals or parameter perturbations, which are state independent, to drive the system from an initial state to a desired target. It is, however, difficult to formulate a general and robust open-loop control framework. It is thus of interest to investigate closed-loop control for complex nonlinear dynamical networks, in which a predesigned feedback loop generates control signals according to the instantaneous state of the system. Closed-loop control thus provides a theoretically relevant and significant alternative to controlling complex nonlinear networks.

In controlling chaos in low-dimensional dynamical systems, both open- and closed-loop controls were extensively investigated. The Ott-Grebogi-Yorke [37] principle, in which small, deliberate, and time-dependent perturbations calculated from measured time series are applied to a parameter or a dynamical variable to keep the system in the vicinity of a target periodic orbit, belongs to the open-loop category. Because of the hallmark of chaos, i.e., sensitive dependence on initial conditions, the control perturbation can be small, and there is great flexibility to switch the target orbit. However, real-time observations of the system are needed, and control can be fragile to external disturbances. The method of Pyragas [38,39] is a closed-loop type of control in which a delayed feedback term is added to the system equations. It does not require real-time observation and analysis of the system, so experimental implementation is greatly facilitated and control can be robust against noise, but the time for control realization is infinite and control flexibility is limited. The developmental history of the field of chaos control provides another motivation for us to consider frameworks as an alternative to open-loop methods for nonlinear network control.

In this Letter, we articulate and analyze a global, finite-time, and closed-loop control framework for complex nonlinear dynamical networks. To ensure that our framework is physically significant, we focus on the control energy and the time required to achieve control and investigate their trade-off. We study how network parameters and structure affect the control time and energy and test the control framework using a variety of real biophysical systems including stem cell differentiation, food webs, random ecosystems, and neuronal networks. Analytically, we derive rigorous upper bounds for both the control energy and time. These results suggest that to develop closed-loop control with optimized control time and energy not only is fundamental to the network control field but also has applied values.

We consider nonlinear dynamical networks described by $\dot{x}_i = f(x_i) + \sum_{i=1}^{N} c_{ij}\mathbf{\Gamma}x_j(t) + \mathbf{u}[\mathbf{x}(t)]B_i$, $1 \leq i \leq N$, where N is the network size, $x_i = [x_{i1}, ..., x_{id}]^\top \in \mathbb{R}^d$ denotes the d-dimensional state variable of the ith node, $\mathbf{x}$ represents the state variables of the whole network, $f \colon \mathbb{R}^d \to \mathbb{R}^d$ is a nonlinear velocity field governing the nodal dynamics and satisfying $\|f(x)\| \leq l\|x\|$ or $|x^\top f(x)| \leq l\|x\|^2$ ($\forall x \in \mathbb{R}^d$)

with a positive constant l, $\boldsymbol{C} = (c_{ij}) \in \mathbb{R}^{N \times N}$ is the coupling matrix determined by the network structure, $\boldsymbol{\Gamma} \in \mathbb{R}^{d \times d}$ describes the internal coupling configuration at each node, $\boldsymbol{u}[\boldsymbol{x}(t)] = [u_i(t)]_{1 \leq i \leq M} \in \mathbb{R}^{d \times M}$ ($M \leq N$) is the closed-loop control protocol to be designed, and $B_i = [b_{i1}, \ldots, b_{iM}]^\top \in \mathbb{R}^M$ ($b_{im} = 0, 1$) characterizes the driving by the controller $\boldsymbol{u}$ to the ith node. Going beyond the existing works on open-loop control of complex networks, where the goal is to drive the system to an instantaneous state, we set the control target to be an *unstable* steady state, which, for mathematical convenience, is assumed to be $x_i = 0$ for all i. For any nontrivial target state, a direct translation can be used to transfer the state to $x_i = 0$.

For a general nonlinear dynamical system, a straightforward approach to realizing closed-loop control [40–42] is to set each component of $\boldsymbol{u}$ as $u_i = -k x_i \triangleq u_i^L$ ($1 \leq i \leq M \leq N$). In principle, this linear feedback controller of strength k is able to steer the dynamics to converge to the target $x_i = 0$, but the time required for convergence is infinite. We thus seek alternative methods [43–46] to achieve a finite control time and robustness against disturbances. A typical form of the feedback controller is $u_i = -k\,\mathrm{sig}(x_i)^\alpha \triangleq u_i^F$, which can drive the system to $x_i = 0$ for all $t \geq T_f^F$ with $T_f^F < \infty$, where $\mathrm{sig}(x_i)^\alpha = [\mathrm{sgn}(x_{i1})|x_{i1}|^\alpha, \ldots, \mathrm{sgn}(x_{id})|x_{id}|^\alpha]^\top$, $\mathrm{sgn}(\cdot)$ is a sign function, k is the control strength, and $\alpha \in (0, 1)$ is the steepness exponent. The mathematical underpinning of the controller u_i^F lies in that the non-Lipschitzian $|\cdot|^\alpha$ at $x_i = 0$ violates the solution uniqueness of the system of coupled differential equations.

To gain physical insights into the control process, we consider the potential function $\mathcal{E}_p^{L,F}(x_i) = \int_0^{x_i} u_i^{L,F} dx_i$, which can be determined from the closed-loop feedback controller. We find that u_i^L is located higher than u_i^F for $|x_i| > 1$, while the opposite occurs for $|x_i| < 1$, as shown in Fig. 1(a). On the potential landscape, the controlled system trajectory can be regarded as a particle moving along some optimal path towards the target $x_i = 0$, the minimum of the potential. The particle experiences a stronger potential force along a path determined by u_i^L (u_i^F) for $|x_i| > 1$ ($|x_i| < 1$). The maximum force occurs for $|x_i| < 1$ and $\alpha \to 0$. In this case, $u_i^F|_{\alpha=0}$ corresponds to a double-valued and closed-loop controller, similar to the classical bang-bang control [47]. The basic principle is then to design two controllers in complementary regions of the phase space. This consideration leads us to propose the following global, compound controller: $u_i = u_i^F \mathcal{I}_{\mathcal{U}} + u_i^L \mathcal{I}_{\mathcal{U}^c} \triangleq u_i^S$, where $1 \leq i \leq M$, the unit ball is defined by $\mathcal{U} = \{\|\boldsymbol{x}\| < 1\}$, $\boldsymbol{x} = [x_1^\top, \ldots, x_N^\top]^\top$, $\|\cdot\|$ denotes an appropriate norm of the underlying vector, $\mathcal{U}^c$ is the complement of $\mathcal{U}$, and $\mathcal{I}$ is the indication function for a given subscript set. The norm can be taken as the L_p or L_∞. To be representative and without the loss of generality, we study the L_2 norms. As shown in Fig. 1(b), the compound controller u_i^S switches from u_i^L to u_i^F when the system enters the unit sphere.
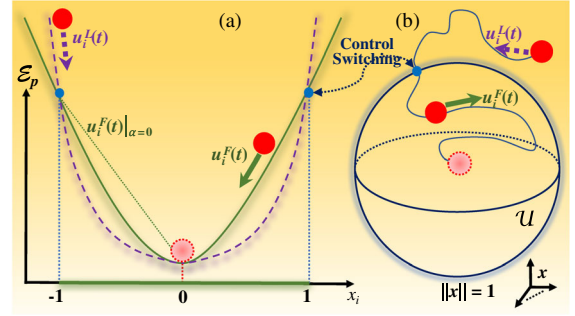

FIG. 1. Physical underpinning of our closed-loop feedback controller. (a) System moving according to the potential function $\mathcal{E}_p^{L,F}$ (dashed curves) underlying closed-loop feedback controllers $u_i^{L,F}$, where u_i^L specifies a linear feedback controller that acts outside of the unit sphere and u_i^F denotes a general feedback controller that is activated once the system is inside the unit sphere. (b) Controlled system trajectory in the phase space by u_i^S, where a control switch occurs when the system crosses the unit sphere $\|\boldsymbol{x}\| = 1$.

We now prove that the controller $\boldsymbol{u}^S = [u_i^S]_{1 \leq i \leq M}$ enables finite-time control and provide an estimate of T_f^S, the time required to achieve control. To be concrete, we set $M = N$, $b_{ii} = 1$, and $b_{im} = 0$ for $i \neq m$. As shown in Fig. 1(b), for $\boldsymbol{x}(0) \notin \mathcal{U}$, the control protocol is set as $u_i^S = u_i^L$. A direct calculation gives $d\|\boldsymbol{x}(t)\|^2/dt \leq -2(k - l - \eta_{\max})\|\boldsymbol{x}(t)\|^2$, where $\eta_{\max}$ is the maximal eigenvalue of the matrix $\boldsymbol{H} \equiv [(\boldsymbol{C} \otimes \boldsymbol{\Gamma})^\top + \boldsymbol{C} \otimes \boldsymbol{\Gamma}]/2$ and $\otimes$ represents the Kronecker product for matrices. Setting $k > l + \eta_{\max}$ when the networked system is outside of the ball $\mathcal{U}$, we get the time instant t^* such that $\boldsymbol{x}(t)|_{t=t^*}$ hits the sphere of $\mathcal{U}$ with $t^* \leq [\ln\|\boldsymbol{x}(0)\|]/\rho$ and $\rho \triangleq k - l - \eta_{\max} > 0$. Once the orbit $\boldsymbol{x}(t)$ enters $\mathcal{U}$ after t^*, because of the dissipation inside $\mathcal{U}$ (see Supplemental Material [48]), the system will never leave it, so that u_i^S becomes u_i^F with the corresponding value k for $t > t^*$, as shown in Fig. 1(b). The dynamical systems theory [48] stipulates that $d\|\boldsymbol{x}(t)\|^2/dt \leq -2\rho\|\boldsymbol{x}(t)\|^{1+\alpha}$ for $t \geq t^*$ and that $\boldsymbol{x}(t) \equiv 0$ for all $t \geq t^* + 1/\rho(1 - \alpha)$. An analogous analysis applies to the case $\boldsymbol{x}(0) \in \mathcal{U}$ with $u_i^S = u_i^F$. The upper bound for T_f^S is then given by

$$T_f^{S_{\mathrm{up}}} = \begin{cases} \frac{1}{\rho}\left(\ln\|\boldsymbol{x}(0)\| + \frac{1}{1-\alpha}\right), & \boldsymbol{x}(0) \notin \mathcal{U}, \\ \|\boldsymbol{x}(0)\|^{1-\alpha}\frac{1}{\rho(1-\alpha)}, & \boldsymbol{x}(0) \in \mathcal{U}, \end{cases} \quad (1)$$

with the condition $\rho > 0$. We see that, for given values of α and $\boldsymbol{x}(0)$ as well as specific network dynamics with l, $\boldsymbol{C}$, and $\boldsymbol{\Gamma}$, the estimation (1) is on the order of $O(1/k)$, where $O(1)$ is a positive and bounded quantity. Accordingly, $\boldsymbol{u}^S$ with a larger value of k can expedite control.

For our controller $\boldsymbol{u}^S$, the required energy cost is [7] $\mathcal{E}_c^S = \int_0^{T_f^S} \sum_{i=1}^N \|u_i^S(t)\|^2 dt$. A lengthy calculation [48] leads to the following upper bound for the energy cost:

$$\mathcal{E}_c^{S_{\mathrm{up}}} = \begin{cases} k^2 \frac{1}{2\rho}\left(1 - \|\boldsymbol{x}(0)\|^{-2} + \frac{2\zeta}{1+\alpha}\right), & \boldsymbol{x}(0) \notin \mathcal{U}, \\ k^2 \frac{\zeta}{\rho(1+\alpha)}\|\boldsymbol{x}(0)\|^{1+\alpha}, & \boldsymbol{x}(0) \in \mathcal{U}, \end{cases} \quad (2)$$

where $\zeta = (Nd)^{1-\alpha}$. Since $\rho \sim k$, $\mathcal{E}_c^S$ is bounded from above by a quantity on the order of $O(k)$. This indicates that, for a given network and given values of α and $\boldsymbol{x}(0)$, increasing k will raise the energy cost. In addition, for fixed values of α and $\boldsymbol{x}(0)$, if k is sufficiently large, increasing l or η_{max} will lead to larger upper bounds for both the control time and energy. For example, for an unweighed and undirected network with $\boldsymbol{\Gamma}$ being an identity matrix, the quantity η_{max} becomes $\lambda_{\mathrm{max}}(\boldsymbol{C})$, so increasing the maximum eigenvalue would demand more time and energy for the $\boldsymbol{u}^S$-driven control to be successful.

Using $\partial_\alpha(\ln T_f^{S_{\mathrm{up}}}) = \ln\|\boldsymbol{x}(0)\|^{-1} + 1/(1-\alpha)$, $\|\boldsymbol{x}(0)\| \leq 1$, and $\alpha \in (0,1)$, we can prove that $T_f^{S_{\mathrm{up}}}$ is an increasing function of α, i.e., $\partial_\alpha(T_f^{S_{\mathrm{up}}}) > 0$, implying that control can be expedited by using a smaller value of the steepness exponent α. In addition, the condition $\partial_\alpha(\mathcal{E}_c^{S_{\mathrm{up}}}) < 0$ implies that smaller values of α lead to higher energy costs. The dependence of the energy on α is consistent with the intuitive, potential-landscape-based physical scenario of control. These results reveal a trade-off between the control time and energy cost for our controller $\boldsymbol{u}^S$ with respect to variations in α or k. For example, consider the index $\mathcal{J}_{\gamma,\beta}(k) = \gamma\lfloor T_f^S\rfloor + \beta\lfloor\mathcal{E}_c^S\rfloor$, where γ and β are adjustable weights determined by the specific system and $\lfloor\cdot\rfloor$ is a normalization function. Since $\mathcal{J}_{\gamma,\beta}(k) \sim O(1/k) + O(k)$, there must exist a number $k_c \gtrsim l + \eta_{\mathrm{max}}$ at which the quantity $\mathcal{J}_{\gamma,\beta}$ reaches its minimum. The optimal control strength is thus given by $k = k_c$ in the sense that control can be achieved in less time with a lower energy cost in terms of the index $\mathcal{J}_{\gamma,\beta}$.

We demonstrate the working of our optimal closed-loop controller $\boldsymbol{u}^S$, its superior performance as compared with the conventional controllers $\boldsymbol{u}^L = [u_i^L]_{1 \leq i \leq M}$, and the corresponding analytic bounds of the control time and energy, using a number of representative real-world complex nonlinear dynamical networks.

Controlling stem cell fate.—We demonstrate that our closed-loop controller can drive two different cell fates to the critical expression level to enable stem cells to remaster their cell fate for cellular differentiation. Specifically, we consider the following network model for hematopoietic stem cells [56], which describes the interaction between two suppressors during cellular differentiation for neutrophil and macrophage cell fate choices [57,58]: $\dot{x}_1 = 0.5 - x_1$, $\dot{x}_2 = 5x_1/[(1+x_1)(1+x_3^4)] - x_2$, $\dot{x}_3 = 5x_4/(1+x_4)(1+x_2^4) - x_3$, $\dot{x}_4 = 0.5/(1+x_2^4) - x_4$, $\dot{x}_5 = [x_1x_4/(1+x_1x_4) + 4x_3/(1+x_3)]/(1+x_2^4) - x_5$, and $\dot{x}_6 = [x_1x_4/(1+x_1x_4) + 4x_2/(1+x_2)]/(1+x_3^4) - x_6$, where $x_{2,3}$ are the expression levels of two lineage-specific counteracting suppressors Gfi-1 and
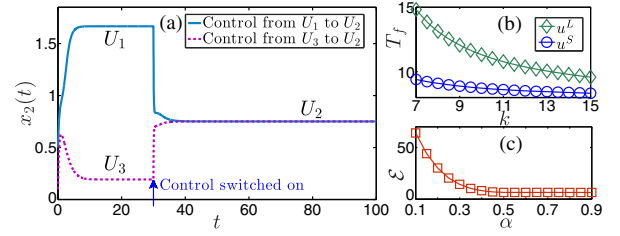

FIG. 2. Controlling a cellular differentiation network model from the steady state $U_1 = (0.5, 1.66, 0.03, 0.06, 0.02, 2.53)$ or $U_3 = (0.5, 0.19, 1.66, 0.50, 2.69, 0.10)$ to the steady state $U_2 = (0.5, 0.75, 1.05, 0.38, 1.69, 0.83)$. (a) Uncontrolled dynamics [for $t \in [0, 30)$] and controlled dynamics (for $t \geq 30$) for the expression levels of suppressor x_2, where $k = 10$ and $\alpha = 0.5$ when u^S is switched on. (b) For $\alpha = 0.5$, the control time versus k for the two controllers $u^{S,L}$. (c) For $k = 10$, the control energy versus α for controller u^S.

Egr(1,2), which are activated by their transcription factors $x_{1,4}$ and simultaneously regulate the downstream genes $x_{5,6}$, respectively. As specified in Fig. 2, the system has three steady states: $U_{1,2,3}$, where $U_{1,3}$ correspond to different cell fates and are stable and U_2 represents a critical expression level connecting the two fates and is unstable. Figure 2(a) shows that initially x_2 of the uncontrolled system converges to the stable steady state U_1 or U_3. From $t = 30$, we apply the finite-time controller $u^S = u^F \mathcal{I}_{\mathcal{U}} + u^L \mathcal{I}_{\mathcal{U}^c}$ with $\mathcal{U} = \{\|\boldsymbol{x} - U_2\| < 1\}$, $u^L = -k(x_2 - U_{22})$, and $u^F = -k\,\mathrm{sgn}(x_2 - U_{22})|x_2 - U_{22}|^\alpha$ to x_2, which is the only variable experimentally accessible [56]. Here, U_{22} is the second component of U_2. The controlled system in either of the stable states is driven rapidly to the critical state U_2, indicating that a finite-time, closed-loop intervention can make the stem cells remaster their cell fate for cellular differentiation. Furthermore, for sufficiently strong control strength k, the converging time with the controller u^S is shorter than that with u^L, as shown in Fig. 2(b). Figure 2(c) shows that, for a fixed value of k, the required control energy decreases with the steepness exponent α, as predicted by our analysis.

Controlling nonlinear ecosystems on food-web networks.—The nonlinear ecological model is described by $\dot{x}_i = x_i(1 - x_i/K_i)(x_i/A_i - 1) \triangleq f(x_i)$, where x_i is the species abundance, f characterizes the logistic growth, and the carrying capacity is K_i. The model includes the Allee effect, where the species is *destined for extinction* if its abundance is lower than a threshold value ($x_i < A_i$) [59–61]. We demonstrate that our control method can successfully restore the system out of extinction to a sustainable state. In particular, for each i, the model has two stable steady states ($x_i = 0$, K_i, corresponding to species extinction and capacity overload, respectively) and one unstable steady state ($x_i = A_i$). To prevent the system from evolving into one of the stable steady states, we choose the control target to be $x_i = A_i$ for all i that represents restoration or sustainment of species to a state with moderate abundance.
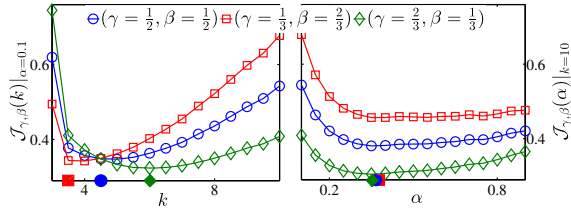
FIG. 3.   Dependence of the optimal control strength or steepness exponent on preferential weights. For the Florida food web, optimal locations of the control indices $\mathcal{J}_{\gamma,\beta}(k)|_{\alpha=0.1}$ and $\mathcal{J}_{\gamma,\beta}(\alpha)|_{k=10}$ versus the weights, as indicated by the markers along the horizontal axis.
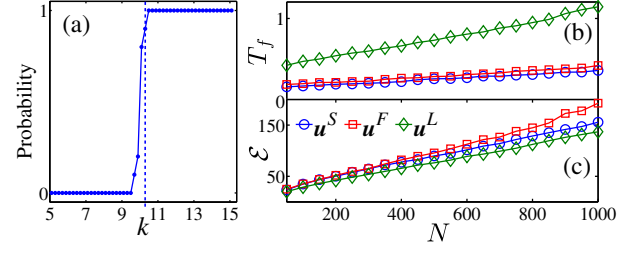

FIG. 4.   For May's classic ecosystems, the probability of successful control versus k (a), where the vertical dashed line corresponds to $\eta_{\max}$, $N = 250$, $P = 0.25$, $\sigma_0 = 1$, $r = 1$, and $\alpha = 0.6$, and the required control time cost (b) and energy cost (c), respectively, with the increase of N for $k = 1.1\eta_{\max}$.

The coupling matrices C are constructed from a large number of real food-web networks [48]. For the three controllers $u^{S,F,L}$, we calculate the respective control time $T_f^{S,F,L}$ required to drive the system into the neighborhood of the target: $|x_i(t) - A_i| \leq 10^{-4}$, $1 \leq i \leq N$. The controller u^S results in the least control time (see Table S1 in [48] for detailed values from all 22 food-web networks).

To verify our analytic prediction of optimal control through the control indices $\mathcal{J}_{\gamma,\beta}$, we use the Florida food web [48] and calculate the indices as a function of k or α. Figure 3 shows that the optimal values of k_c and α_c depend on the combination of the preferential weights (γ, β), which agree well with the respective analytic results. Simulations further reveal that the optimal value k_c is more sensitive to the choice of the preferential weights than α_c, which is reasonable as decreasing the control time tends to make the value of k_c larger.

Controlling complex random ecosystems.—Consider a general ecosystem described by $\dot{x} = Cx$, where each species x_i is one-dimensional, $C = (c_{ij})_{N \times N}$ describes the random mutual interactions with $c_{ii} = -r$, and N is the population size. Three types of random matrices C were studied extensively, which correspond to three typical ecosystems: (a) May's classic ecosystem [62], where, with probability P, the off-diagonal elements c_{ij} are set as mutually independent Gaussian random variables $\mathcal{N}(0, \sigma_0^2)$ and the probability for the elements to be zero is $(1 - P)$; (b) a mixed ecosystem of competition and mutualism [63], where the off-diagonal elements c_{ij} and c_{ji} have the same sign, which are drawn from the distribution $(\pm|\mathcal{Y}|, \pm|\mathcal{Y}|)$ with probability P and are zero with probability $(1 - P)$; and (c) the predator-prey (PP) ecosystem [63], where c_{ij} and c_{ji} have the opposite signs and are from the distribution $(\pm|\mathcal{Y}|, \mp|\mathcal{Y}|)$. As either N or the variance of C's elements increases, all three ecosystems eventually become unstable, reflecting the instability of a certain steady state in the original ecosystem from which the linear random system was derived [62,63].

We employ u^S to control the ecosystems, which becomes a particular case of our general nonlinear network control

framework with $l = 0, \Gamma = 1, b_{ii} = 1$, and all other $b_{im} = 0$. To achieve finite-time control, we estimate the maximal eigenvalue $\eta_{\max}$ of $H = (C^\top + C)/2$ (see Supplemental Material). For May's classic ecosystem, the well-known semicircle law for random matrices stipulates that H's eigenvalues are located in $[-\sqrt{2NP}\sigma_0 - r, \sqrt{2NP}\sigma_0 - r]$ as $N \to \infty$ (Supplemental Material). According to Eq. (1), to realize finite-time control requires $k > \eta_{\max} = \sqrt{2NP}\sigma_0 - r$ (condition A). As shown in Fig. 4(a), successful control is achieved for sufficiently large values of k. However, from the estimates of the control time and energy [Eqs. (1) and (2), respectively], we see that, for a fixed large value of k, an increase in either N or σ_0 slows down the control and consumes more energy, eventually violating condition A and causing the control to fail, as shown in Figs. 4(b) and 4(c). While the controller u^S requires the least control time among the three available controllers, for a large system size the corresponding energy cost is not necessarily minimum.

For the mixed ecosystem with $\mathcal{Y} \sim \mathcal{N}(0, \sigma_0^2)$, from H's eigenvalue distribution obtained in Ref. [48], we have $k > \sqrt{2NP(1 + 2/\pi)}\sigma_0 - r$ (condition B) that ensures finite-time control in the probabilistic sense. Similarly for the PP system, we require $k > \sqrt{2NP(1 - 2/\pi)}\sigma_0 - r$ (condition C). Overall, conditions A–C reveal a *hierarchy* where the PP, May's classic, and mixed ecosystems require the weakest, intermediate, and strongest control strength k, respectively. The control time for the three systems can be made finite and identical, because the respective choices of the k value can result in the same value of ρ in Eq. (1). In spite of this, the ordering of the control energy for the three types of ecosystems cannot be altered, because k appears still in Eq. (2) in addition to ρ.

Akin to the previous example of controlling stem cell fate via only one suppressor, we apply our finite-time controller to different numbers of species in the ecosystem with an undirected scale-free coupling matrix C, which reveals a high flexibility of our controller (see [48]).

In summary, we develop a closed-loop control framework for nonlinear dynamical networks to drive the system to a desired unstable steady state in a finite time and with a

predictable energy. Because of the closed-loop nature and high flexibility of the controller, it is suitable for the experimental control of nonlinear networks. We obtain physical and mathematical understandings of the trade-off between the control time and energy. Our closed-loop controller is also effective for realizing synchronization in nonlinear neuronal networks (see [48]). While the issue of optimal energy associated with closed-loop control and single- or two-layer structure has been investigated [64,65], prior to our work a closed-loop control scheme for nonlinear dynamical networks with both optimal time and energy had not been achieved. Our work provides a base for developing a general, physically realizable closed-loop control scheme for complex nonlinear networks with completely unknown steady states.

Y.-Z. S. and S.-Y. L. contributed equally to this work.

---

*wlin@fudan.edu.cn

[1] A. Lombardi and M. Hörnquist, Phys. Rev. E **75**, 056110 (2007).
[2] B. Liu, T. Chu, L. Wang, and G. Xie, IEEE Trans. Autom. Control **53**, 1009 (2008).
[3] A. Rahmani, M. Ji, M. Mesbahi, and M. Egerstedt, SIAM J. Control Optim. **48**, 162 (2009).
[4] Y.-Y. Liu, J.-J. Slotine, and A.-L. Barabási, Nature (London) **473**, 167 (2011).
[5] W.-X. Wang, X. Ni, Y.-C. Lai, and C. Grebogi, Phys. Rev. E **85**, 026115 (2012).
[6] J. C. Nacher and T. Akutsu, New J. Phys. **14**, 073005 (2012).
[7] G. Yan, J. Ren, Y.-C. Lai, C.-H. Lai, and B. Li, Phys. Rev. Lett. **108**, 218703 (2012).
[8] T. Nepusz and T. Vicsek, Nat. Phys. **8**, 568 (2012).
[9] Y.-Y. Liu, J.-J. Slotine, and A.-L. Barabási, Proc. Natl. Acad. Sci. U.S.A. **110**, 2460 (2013).
[10] Z.-Z. Yuan, C. Zhao, Z.-R. Di, W.-X. Wang, and Y.-C. Lai, Nat. Commun. **4**, 2447 (2013).
[11] T. Jia, Y.-Y. Liu, E. Csóka, M. Pósfai, J.-J. Slotine, and A.-L. Barabási, Nat. Commun. **4**, 3002 (2013).
[12] D. Delpini, S. Battiston, M. Riccaboni, G. Gabbi, F. Pammolli, and G. Caldarelli, Sci. Rep. **3**, 1626 (2013).
[13] J. C. Nacher and T. Akutsu, Sci. Rep. **3**, 1647 (2013).
[14] G. Menichetti, L. DallAsta, and G. Bianconi, Phys. Rev. Lett. **113**, 078701 (2014).
[15] J. Ruths and D. Ruths, Science **343**, 1373 (2014).
[16] S. Wuchty, Proc. Natl. Acad. Sci. U.S.A. **111**, 7156 (2014).

[17] Z.-Z. Yuan, C. Zhao, W.-X. Wang, Z.-R. Di, and Y.-C. Lai, New J. Phys. **16**, 103036 (2014).
[18] F. Pasqualetti, S. Zampieri, and F. Bullo, IEEE Trans. Control Netw. Syst. **1**, 40 (2014).
[19] Y.-D. Xiao, S.-Y. Lao, L.-L. Hou, and L. Bai, Phys. Rev. E **90**, 042804 (2014).
[20] F. Sorrentino, Chaos **17**, 033101 (2007).
[21] F.-X. Wu, L. Wu, J.-X. Wang, J. Liu, and L.-N. Chen, Sci. Rep. **4**, 4819 (2015).
[22] A. J. Whalen, S. N. Brennan, T. D. Sauer, and S. J. Schiff, Phys. Rev. X **5**, 011005 (2015).
[23] J. C. Nacher and T. Akutsu, Phys. Rev. E **91**, 012826 (2015).
[24] T. H. Summers, F. L. Cortesi, and J. Lygeros, IEEE Trans. Control Netw. Syst. **3**, 91 (2015).
[25] Y.-Y. Liu and A.-L. Barabási, Rev. Mod. Phys. **88**, 035006 (2016).
[26] Y.-Z. Chen, L.-Z. Wang, W.-X. Wang, and Y.-C. Lai, R. Soc. Open Sci. **3**, 160064 (2016).
[27] L.-Z. Wang, Y.-Z. Chen, W.-X. Wang, and Y.-C. Lai, Sci. Rep. **7**, 40198 (2017).
[28] X. F. Wang and G. Chen, Physica A (Amsterdam) **310**, 521 (2002).
[29] X. Li, X. F. Wang, and G. Chen, IEEE Trans. Circuits Syst. I **51**, 2074 (2004).
[30] F. Sorrentino, M. di Bernardo, F. Garofalo, and G. Chen, Phys. Rev. E **75**, 046103 (2007).
[31] W. Yu, G. Chen, and J. Lü, Automatica **45**, 429 (2009).
[32] B. Fiedler, A. Mochizuki, G. Kurosawa, and D. Saito, J. Dyn. Differ. Equ. **25**, 563 (2013).
[33] A. Mochizuki, B. Fiedler, G. Kurosawa, and D. Saito, J. Theor. Biol. **335**, 130 (2013).
[34] D. K. Wells, W. L. Kath, and A. E. Motter, Phys. Rev. X **5**, 031036 (2015).
[35] L.-Z. Wang, R.-Q. Su, Z.-G. Huang, X. Wang, W.-X. Wang, C. Grebogi, and Y.-C. Lai, Nat. Commun. **7**, 11323 (2016).
[36] J. G. T. Zanudo, G. Yang, and R. Albert, Proc. Natl. Acad. Sci. U.S.A. **114**, 7234 (2017).
[37] E. Ott, C. Grebogi, and J. A. Yorke, Phys. Rev. Lett. **64**, 1196 (1990).
[38] K. Pyragas, Phys. Lett. A **170**, 421 (1992).
[39] K. Pyragas, Phil. Trans. R. Soc. A **364**, 2309 (2006).
[40] W. Lin, Phys. Lett. A **372**, 3195 (2008).
[41] Y. Wu and W. Lin, Phys. Lett. A **375**, 3279 (2011).
[42] H. Ma, D. W. C. Ho, Y.-C. Lai, and W. Lin, Phys. Rev. E **92**, 042902 (2015).
[43] S. P. Bhat and D. S. Bernstein, SIAM J. Control Optim. **38**, 751 (2000).
[44] F. Amato, M. Ariola, and C. Cosentino, IEEE Trans. Autom. Control **55**, 1003 (2010).
[45] B. Xu and W. Lin, Int. J. Bifurcation Chaos Appl. Sci. Eng. **25**, 1550166 (2015).
[46] H. Rios, D. Efimov, J. A. Moreno, W. Perruquetti, and J. G. Rueda-Escobedo, IEEE Trans. Autom. Control **PP**, 1 (2017).
[47] W. Fleming and R. Rishel, *Deterministic and Stochastic Optimal Control* (Springer, New York, 1975).
[48] See Supplemental Material at http://link.aps.org/supplemental/10.1103/PhysRevLett.119.198301 for analytical estimations of upper bounds for the control time and energy cost, data information and convergence times for

controlling food-web networks, the numerical validation of control flexibility, and the realization of finite-time synchronization in coupled spiking neuronal models, which includes Refs. [26,27,49–55].

[49] G. H. Hardy, J. E. Littlewood, and G. Pólya, *Inequalities* (Cambridge University Press, Cambridge, England, 1988).

[50] W. Rudin, *Functional Analysis* (McGraw-Hill Science, Singapore, 1991).

[51] V. Lakshmikantham and S. Leela, *Differential and Integral Inequalities* (Academic, New York, 1969).

[52] E. P. Wigner, Ann. Math. **67,** 325 (1958).

[53] G. W. Anderson, A. Guonnet, and O. Zeitouni, *An Introduction to Random Matrices* (Cambridge University Press, Cambridge, England, 2009).

[54] A.-L. Barabási and R. Albert, Science **286,** 509 (1999).

[55] J. L. Hindmarsh and R. M. Rose, Nature (London) **296,** 162 (1982).

[56] P. Laslo, C. J. Spooner, A. Warmflash, D. W. Lancki, H.-J. Lee, R. Sciammas, B. N. Gantner, A. R. Dinner, and H. Singh, Cell **126,** 755 (2006).

[57] N. Radde, Bioinformatics **26,** 2874 (2010).

[58] N. Radde, BMC Syst. Biol. **6,** 57 (2012).

[59] J. N. Holland, D. L. DeAngelis, and J. L. Bronstein, Am. Nat. **159,** 231 (2002).

[60] C. Hui, Ecol. Model. **192,** 317 (2006).

[61] W. C. Allee, O. Park, A. E. Emerson, T. Park, and K. P. Schmidt, *Principles of Animal Ecology*, 1st ed. (W. B. Saunders, London, 1949).

[62] R. M. May, Nature (London) **238,** 413 (1972).

[63] S. Allesina and S. Tang, Nature (London) **483,** 205 (2012).

[64] M. Ellisa and P. D. Christofides, Automatica **50,** 2561 (2014).

[65] I. Michailidis, S. Baldi, E. B. Kosmatopoulos, and P. A. Ioannou, IEEE Trans. Autom. Control (to be published).

Supplementary Information for

Closed-loop control of complex nonlinear networks: A tradeoff between time and energy

Yong-Zheng Sun, Si-Yang Leng, Ying-Cheng Lai, Celso Grebogi, and Wei Lin

Corresponding author: Wei Lin (wlin@fudan.edu.cn)

CONTENTS

I. UPPER BOUNDS FOR CONTROL TIME AND ENERGY COST

We provide mathematical estimates of the upper bounds for control time and the associated energy cost with the proposed closed-loop controller $\boldsymbol{u}^S$.

A. Preliminaries

We list two Lemmas that will be used in our analysis.

Lemma S1.1 ([1]). *Let $\xi_1, \xi_2, \ldots, \xi_n \geq 0$ and $0 < p < 1$. The following inequality holds:*

$$\sum_{i=1}^{n} \xi_i^p \geq \left(\sum_{i=1}^{n} \xi_i \right)^p.$$

Lemma S1.2 ([2]). *For any $0 < q \leq p$, there exist two positive numbers $\zeta_{1,2}$ such that*

$$\zeta_1 \| \cdot \|_p \leq \| \cdot \|_q \leq \zeta_2 \| \cdot \|_p,$$

where $\| \cdot \|_h$ ($h = p, q$) is the L_h-norm for the n-dimensional space $\mathbb{R}^n$. Specifically, $\zeta_1 = 1$ and $\zeta_2 = n^{\frac{1}{q} - \frac{1}{p}}$.

B. Estimate of control time

For the general closed-loop controlled network dynamics in the main text, we introduce the following Lyapunov function:

$$V(\boldsymbol{x}) = \sum_{i=1}^{N} x_i^\top x_i = \sum_{i=1}^{N} \|x_i\|^2 = \|\boldsymbol{x}\|^2, \tag{S1.1}$$

where $\boldsymbol{x} = \left[x_1^\top, \cdots, x_N^\top \right]^\top \in \mathbb{R}^{Nd}$ and $\| \cdot \|$ represents the L_2-norm of the given vector. We assume $\boldsymbol{x}(0) \notin \mathcal{U} = \{ \|\boldsymbol{x}(0)\| < 1 \}$. Differentiating the function V along a typical trajectory of the system, we obtain

$$\frac{\mathrm{d}V}{\mathrm{d}t} = 2\sum_{i=1}^{N} x_i^\top f(x_i) + 2\sum_{i=1}^{N} x_i^\top \sum_{j=1}^{N} c_{ij} \Gamma x_j - 2k \sum_{i=1}^{N} x_i^\top x_i \tag{S1.2}$$

$$\leq 2(l-k) \sum_{i=1}^{N} x_i^\top x_i - 2\boldsymbol{x}^\top \boldsymbol{H} \boldsymbol{x} \leq -2(k - l - \eta_{\max}) V(t),$$

where $\boldsymbol{H} \equiv \frac{1}{2} \left[(\boldsymbol{C} \otimes \boldsymbol{\Gamma})^\top + \boldsymbol{C} \otimes \boldsymbol{\Gamma} \right]$ is a matrix and $\eta_{\max}$ is its maximum eigenvalue. The global Lipschitz condition on f can be relaxed to the one-sided uniform Lipschitz condition (a function f is said to be one-sided uniformly Lipschitzian if for some $l > 0$, we have $|x^\top f(x)| \leq l\|x\|^2$ for all $x \in \mathbb{R}^n$). Choosing $k > l + \eta_{\max}$ and integrating the differential inequality (S1.2) from 0 to t, we get $V[(\boldsymbol{x}(t)] = \|\boldsymbol{x}(t)\|^2$, which is circumscribed by an exponentially decreasing quantity. We thus have $V(\boldsymbol{x}(t^*)) = 1$ and

$$\|\boldsymbol{x}(t^*)\| = 1 \text{ with } t^* \leq \frac{\ln \|\boldsymbol{x}(0)\|}{\rho} > 0, \tag{S1.3}$$

2

where $\rho = k - l - \eta_{\max}$ (as defined in the main text).

We next prove that $\|\boldsymbol{x}(t)\| < 1$ for all $t \in (t^*, +\infty)$. Intuitively, this is a result of *system dissipation*. The proof is carried out by contradiction. Specifically, assume this is not the case. We can then obtain the first time instant at which the trajectory $\boldsymbol{x}(t)$, after entering the unit ball $\mathcal{U}$, hits the ball again. Denote this time by

$$t' = \inf \left\{ t \in [\hat{t}, t_1) \,\Big|\, \|\boldsymbol{x}(t)\| = 1 \right\},$$

where the time instants $\hat{t}$ and t_1 satisfy $\|\boldsymbol{x}(t)\| < 1$ with $t^* < t < \hat{t} < t' < t_1 < +\infty$. All the time instants can be found because of the continuity of the trajectory $\boldsymbol{x}(t)$ and the assumption that $\boldsymbol{x}(t)$ can hit the unit ball. For $t \in [\hat{t}, t')$, taking the derivative of $V(t)$ with respect to t yields

$$
\begin{aligned}
\frac{\mathrm{d}V}{\mathrm{d}t} &= 2\sum_{i=1}^{N} x_i^\top f(x_i) + 2\sum_{i=1}^{N} x_i^\top \sum_{j=1}^{N} c_{ij}\Gamma x_j - 2k \sum_{i=1}^{N} x_i^\top \mathrm{sig}(x_i)^\alpha \\
&\leq 2(l + \eta_{\max})\boldsymbol{x}^\top \boldsymbol{x} - 2k \sum_{i=1}^{N} x_i^\top \mathrm{sig}(x_i)^\alpha.
\end{aligned}
\tag{S1.4}
$$

From Lemma S1.1, we have

$$\sum_{i=1}^{N} x_i^\top \mathrm{sig}(x_i)^\alpha = \sum_{i=1}^{N}\sum_{j=1}^{d} |x_{ij}|^{\alpha+1} \geq \left(\sum_{i=1}^{N}\sum_{j=1}^{d} |x_{ij}|^2 \right)^{\frac{\alpha+1}{2}},$$

which gives a further estimation for dV/dt:

$$\frac{\mathrm{d}V}{\mathrm{d}t} \leq 2(l + \eta_{\max})V(t) - 2k\left[V(t)\right]^{\frac{\alpha+1}{2}}.
\tag{S1.5}$$

Since $V(t) = \|\boldsymbol{x}(t)\|^2 \leq 1$ for all $t \in [\hat{t}, t')$, we have $V(t) \leq V^{\frac{\alpha+1}{2}}(t)$ for all $t \in [\hat{t}, t')$. Hence, the estimation in (S1.5) can be refined as:

$$\frac{\mathrm{d}V}{\mathrm{d}t} \leq -2\rho V^{\frac{\alpha+1}{2}}(t), \quad \text{for all } t \in [\hat{t}, t').
\tag{S1.6}$$

This implies $\mathrm{d}V/\mathrm{d}t \leq 0$ for all $t \in [\hat{t}, t')$, so we have

$$1 > \|\boldsymbol{x}(\hat{t})\|^2 = V[\boldsymbol{x}(\hat{t})] \geq V[\boldsymbol{x}(t)]$$

for all $t \in [\hat{t}, t')$. In the limit $t \to t'$, we have $1 > V(\boldsymbol{x}(\hat{t})) \geq V(\boldsymbol{x}(t')) = 1$. This is a contradiction, which implies that for all $t \in (t^*, t_1)$, $\boldsymbol{x}(t) \in \mathcal{U}$ holds, where t_1 can be extended to $+\infty$.

We can now prove that the trajectory $\boldsymbol{x}(t)$ of the general nonlinear network system in the main text approaches the desired target within a finite-time duration in $(t^*, +\infty)$. In particular, from the estimation in (S1.6) and the theory of differential inequalities [3], we have $V(t) \leq W(t)$, where $t \in (t^*, +\infty)$ and $W(t)$ satisfies the following equation:

$$\frac{\mathrm{d}W}{\mathrm{d}t} = -2\rho W^{\frac{\alpha+1}{2}}(t), \quad \text{for all } t > t^*,
\tag{S1.7}$$

with the initial condition $W(t^*) = V(t^*) = 1$. From (S1.7), we have

$$\frac{1}{1-\alpha} W^{\frac{1-\alpha}{2}}(t) = -\rho t + c_0, \quad \text{for all } t > t^*, \tag{S1.8}$$

where $c_0 = \rho t^* + \frac{1}{1-\alpha} V^{\frac{1-\alpha}{2}}(t^*)$ and t^* is defined in (S1.3). From (S1.8), we have

$$V(t) \leq W(t) = [(1-\alpha)(-\rho t + c_0)]^{\frac{2}{1-\alpha}}. \tag{S1.9}$$

Letting $W(t) = 0$, we obtain the upper bound for the time T_f^S to achieve control:

$$T_f^S \leq t^* + \frac{\|\boldsymbol{x}(t^*)\|^{1-\alpha}}{\rho(1-\alpha)} = t^* + \frac{1}{\rho(1-\alpha)}.$$

For the case of $\boldsymbol{x}(0) \in \mathcal{U}$, a similar argument leads to the upper bound for T_f^S as

$$T_f^S \leq \frac{\|\boldsymbol{x}(0)\|^{1-\alpha}}{\rho(1-\alpha)}.$$

The estimated upper bound for T_f^S can thus be summarized as

$$T_f^{S_{\text{up}}} = \begin{cases} \frac{1}{\rho}\ln\|\boldsymbol{x}(0)\| + \frac{1}{\rho(1-\alpha)}, & \boldsymbol{x}(0) \notin \mathcal{U}, \\ \frac{1}{\rho(1-\alpha)}\|\boldsymbol{x}(0)\|^{1-\alpha}, & \boldsymbol{x}(0) \in \mathcal{U}. \end{cases} \tag{S1.10}$$

For the special case of controlled linear network dynamics $\dot{\boldsymbol{x}} = \boldsymbol{C}\boldsymbol{x} + [\boldsymbol{u}^S]^\top$, we set $l = 0$, $\boldsymbol{\Gamma} = 1$, $b_{ii} = 1$, and all other $b_{im} = 0$. The upper bound of the required control time can be estimated as

$$T_f^{S_{\text{up}}} = \begin{cases} \frac{1}{\rho}\ln\|\boldsymbol{x}(0)\| + \frac{1}{(k-\mu_{\text{max}})(1-\alpha)}, & \boldsymbol{x}(0) \notin \mathcal{U}, \\ \frac{1}{(k-\mu_{\text{max}})(1-\alpha)}\|\boldsymbol{x}(0)\|^{1-\alpha}, & \boldsymbol{x}(0) \in \mathcal{U}, \end{cases}$$

where μ_{max} is the maximal eigenvalue of the matrix $\frac{1}{2}[\boldsymbol{C} + \boldsymbol{C}^\top]$.

C. Estimate of control energy cost

Case 1: $\boldsymbol{x}(0) \notin \mathcal{U}.$ From the definition in the main text, the energy cost is given by

$$\mathcal{E}_c^S = \int_0^{T_f} \sum_{i=1}^N \|u_i^S(t)\|^2 \, \mathrm{d}t = \int_0^{t^*} \sum_{i=1}^N \|u_i^L(t)\|^2 \, \mathrm{d}t + \int_{t^*}^{T_f} \sum_{i=1}^N \|u_i^F(t)\|^2 \, \mathrm{d}t.$$

Outside the unit ball $\mathcal{U}$, the energy cost can be estimated as

$$\int_0^{t^*} \sum_{i=1}^N \|u_i^L(t)\|^2 \, \mathrm{d}t = k^2 \int_0^{t^*} \|\boldsymbol{x}(t)\|^2 \mathrm{d}t = k^2 \int_0^{t^*} V(t)\mathrm{d}t.$$

From the estimate (S1.2), we get

$$\begin{aligned} k^2 \int_0^{t^*} V(t)\mathrm{d}t &\leq k^2 V(0) \int_0^{t^*} \mathrm{e}^{-2\rho t}\mathrm{d}t \\ &= k^2 V(0) \left(-\frac{1}{2\rho}\mathrm{e}^{-2\rho t^*} + \frac{1}{2\rho}\right) k^2 \left[\frac{1}{2\rho} - \frac{1}{2\rho\|\boldsymbol{x}(0)\|^2}\right]. \end{aligned} \tag{S1.11}$$

Note that

$$\sum_{i=1}^{N} \left\| u_i^F(t) \right\|^2 = k^2 \sum_{i=1}^{N} \sum_{j=1}^{d} |x_{ij}(t)|^{2\alpha} = k^2 \left\| \boldsymbol{x}(t) \right\|_{2\alpha}^{2\alpha} \leq \zeta k^2 \left\| \boldsymbol{x}(t) \right\|^{2\alpha} = \zeta k^2 V^\alpha(t),$$

where the inequality follows from Lemma S1.2 and $\zeta = (\zeta_2)^{2\alpha} = \left[(Nd)^{\frac{1}{2\alpha} - \frac{1}{2}} \right]^{2\alpha} = (Nd)^{1-\alpha}$. This, with (S1.9), gives an estimate of the energy cost inside $\mathcal{U}$:

$$\int_{t^*}^{T_f} \sum_{i=1}^{N} \left\| u_i^F(t) \right\|^2 \mathrm{d}t \leq \zeta k^2 \int_{t^*}^{T_f} V^\alpha(t)\mathrm{d}t \leq \zeta k^2 \int_{t^*}^{T_f} (1-\alpha)^{\frac{2}{1-\alpha}} (-\rho t + c_0)^{\frac{2\alpha}{1-\alpha}} \mathrm{d}t$$

$$= \zeta k^2 \frac{1}{\rho(1+\alpha)} (1-\alpha)^{\frac{1+\alpha}{1-\alpha}} \left[(-\rho t^* + c_0)^{\frac{1+\alpha}{1-\alpha}} - (-\rho T_f + c_0)^{\frac{1+\alpha}{1-\alpha}} \right], \tag{S1.12}$$

where $c_0 = 1/(1-\alpha)$. Substituting the estimation of T_f into (S1.12), we get

$$\int_{t^*}^{T_f} \sum_{i=1}^{N} \left\| u_i^F(t) \right\|^2 \mathrm{d}t \leq \zeta k^2 \frac{1}{\rho(1+\alpha)}. \tag{S1.13}$$

Finally, from (S1.11) and (S1.13), we obtain the upper bound estimate of the energy-cost as

$$\mathcal{E}_c^{S_{\mathrm{up}}} = k^2 \frac{1}{2\rho} \left[1 - \left\| \boldsymbol{x}(0) \right\|^{-2} + \frac{2\zeta}{1+\alpha} \right].$$

Case 2: $\boldsymbol{x}(0) \in \mathcal{U}$. The energy cost is

$$\mathcal{E}_c = \int_0^{T_f} \sum_{i=1}^{N} \left\| u_i^F(t) \right\|^2 \mathrm{d}t \leq \zeta k^2 \int_0^{T_f} V^\alpha(t)\mathrm{d}t.$$

Following the argument for Case 1, we get

$$\mathcal{E}_c \leq \zeta k^2 \int_0^{T_f} (1-\alpha)^{\frac{2}{1-\alpha}} (-\rho t + \tilde{c}_0)^{\frac{2\alpha}{1-\alpha}} \mathrm{d}t$$

$$= \zeta k^2 \frac{1}{\rho(1+\alpha)} (1-\alpha)^{\frac{1+\alpha}{1-\alpha}} \left[(\tilde{c}_0)^{\frac{1+\alpha}{1-\alpha}} - (-\rho T_f + \tilde{c}_0)^{\frac{1+\alpha}{1-\alpha}} \right],$$

where $\tilde{c}_0 = \frac{1}{1-\alpha} \left\| \boldsymbol{x}(0) \right\|^{1-\alpha}$. From the estimated T_f in (S1.10), we get

$$\mathcal{E}_c^{S_{\mathrm{up}}} = \frac{\zeta k^2}{\rho(1+\alpha)} \left\| \boldsymbol{x}(0) \right\|^{1+\alpha}.$$

To summarize, the analytical estimate for the upper bound of the energy cost is given by

$$\mathcal{E}_c^{S_{\mathrm{up}}} = \begin{cases} k^2 \frac{1}{2\rho} \left[1 - \left\| \boldsymbol{x}(0) \right\|^{-2} + \frac{2\zeta}{1+\alpha} \right], & \boldsymbol{x}(0) \notin \mathcal{U}; \\ k^2 \frac{\zeta}{\rho(1+\alpha)} \left\| \boldsymbol{x}(0) \right\|^{1+\alpha}, & \boldsymbol{x}(0) \in \mathcal{U}, \end{cases}$$

where $\zeta = (Nd)^{1-\alpha}$.

TABLE S1. Results of controlling 22 nonlinear food-web networks with the controllers $\boldsymbol{u}^{S,F,L}$, where $K_i = 5$, $A_i = 1$, $k = 2$, and $\alpha = \frac{1}{2}$. The dynamical variables in the initial state are chosen randomly from the interval $[0, 5]$. Each data point is the result of averaging 100 control realizations.

Food-web name	# of nodes	# of edges	T_f^S	T_f^F	T_f^L
Chesapeake	39	177	2.88	5.45	7.32
ChesLower	37	166	2.84	5.37	7.05
ChesMiddle	37	203	2.85	5.34	6.96
ChesUpper	37	206	2.90	5.43	7.30
CrystalC	24	125	2.91	5.49	7.34
CrystalD	24	100	2.91	5.48	7.15
Everglades	69	916	2.92	5.50	7.35
Florida	128	2106	2.92	5.50	7.25
Maspalomas	24	82	2.80	5.27	7.48
Michigan	39	221	2.91	5.49	7.18
Mondego	46	400	2.90	5.44	7.18
Narragan	35	220	2.94	5.52	7.50
Rhode	20	53	2.90	5.46	7.22
St. Marks	54	356	2.87	5.37	7.28
baydry	128	2137	2.92	5.50	7.36
baywet	128	2106	2.92	5.49	7.06
cypdry	71	640	2.90	5.47	7.16
cypwet	71	631	2.90	5.48	7.05
gramdry	69	915	2.92	5.50	7.28
gramwet	69	916	2.93	5.52	7.30
Mangrove Dry	97	1491	2.92	5.50	7.28
Mangrove Wet	97	1492	2.93	5.52	7.31

II.   CONTROLLING FOOD-WEB NETWORKS: DATA AND ANALYSES

All the results on control time for controlling the 22 food-web networks are shown in Tab. S1. The food-web data are from the website:

http://vlado.fmf.uni-lj.si/pub/networks/data/bio/foodweb/foodweb.htm

As shown in Fig. S1, the required control time and energy cost for controlling the Florida food-web network exhibit exactly the opposite trends with increasing k and α. This, together with Fig. 2 in the main text, reveals a control trade-off between the time and the energy cost inherent to the controller $\boldsymbol{u}^S$.

III.   EIGENVALUE DISTRIBUTIONS OF ECOLOGICAL NETWORKS

Here we prove that, for May's classic ecosystem, $\boldsymbol{H}$'s eigenvalues are distributed in the interval $\left[-r - \sqrt{2NP}\sigma_0, -r + \sqrt{2NP}\sigma_0 \right]$ in a probabilistic sense as $N \to \infty$. Thus, to realize

control requires
$$k > \eta_{\max} = \sqrt{2NP}\sigma_0 - r \quad \textbf{(Condition-A)}.$$

For the mixed ecosystem, $\boldsymbol{H}$'s eigenvalues are distributed in the interval
$$\left[-\sqrt{2NP[\mathbb{D}(\mathcal{Y}) + \mathbb{E}^2(|\mathcal{Y}|)]} - r, \ \sqrt{2NP[\mathbb{D}(\mathcal{Y}) + \mathbb{E}^2(|\mathcal{Y}|)]} - r \right]$$

as $N \to \infty$. Particularly, for $\mathcal{Y} \sim \mathcal{N}(0, \sigma_0^2)$, this interval becomes $\left[-\sqrt{2NP(1 + 2/\pi)}\sigma_0 - r, \sqrt{2NP(1 + 2/\pi)}\sigma_0 - r \right]$, yielding

$$k > \sqrt{2NP(1 + 2/\pi)}\sigma_0 - r \quad \textbf{(Condition-B)}$$

which ensures finite-time control in the probabilistic sense. For the PP system, we have

$$k > \sqrt{2NP(1 - 2/\pi)}\sigma_0 - r \quad \textbf{(Condition-C)}$$

for realizing control in the probabilistic sense.

A. Wigner semicircle law

Lemma S3.1 (Semicircle Law [4, 5]). *Let $\{Z_{i,j}\}_{1 \leq i < j}$ and $\{Y_i\}_{1 \leq i}$ be two independent families of i.i.d., zero mean, and real-valued random variables with $\mathbb{E}(Z_{1,2}^2) = 1$. Further, assume that for all integers $k \geq 1$,*
$$r_k \triangleq \max\left\{ \mathbb{E}|Z_{1,2}|^k, \mathbb{E}|Y_1|^k \right\} < \infty.$$
Set the elements of the symmetric $N \times N$ matrix $\boldsymbol{X}_N$ as:
$$\boldsymbol{X}_N(i, j) = \boldsymbol{X}_N(j, i) = \begin{cases} Z_{i,j}/\sqrt{N}, & i < j, \\ Y_i/\sqrt{N}, & i = j. \end{cases}$$
Let the empirical measure be $L_N = \frac{1}{N}\sum_{i=1}^N \delta_{\lambda_i}$, where λ_i $(1 \leq i \leq N)$ are the real eigenvalues of $\boldsymbol{X}_N$. Let the standard semicircle distribution be the probability distribution $\sigma(x)\mathrm{d}x$ on $\mathbb{R}$ with the density
$$\sigma(x) = \frac{1}{2\pi}\sqrt{4 - x^2}\mathcal{I}_{|x|<2},$$
where $\mathcal{I}$ is the indication function of a given set. Then, L_N converges weakly probabilistically to the standard semicircle distribution as $N \to \infty$.

B. Eigenvalue distributions of ecological networks

May's classic ecosystem. For this system, we have $c_{ii} = -r$ and the off-diagonal elements c_{ij} are mutually independent random variables that obey the Gaussian normal distribution $\mathcal{N}(0, \sigma_0^2)$ with probability P and are zero with probability $1 - P$. Denote each element of the symmetric matrix $\boldsymbol{H} = \frac{1}{2}\left[\boldsymbol{C} + \boldsymbol{C}^\top\right]$ by $\xi_{ij} = \frac{1}{2}(c_{ij} + c_{ji})$. The expectation is $\mathbb{E}(\xi_{ij}) = \frac{1}{2}\left[\mathbb{E}(c_{ij}) + \mathbb{E}(c_{ji})\right] = 0$ and the variance is given by

$$\mathbb{D}(\xi_{ij}) = \frac{1}{4}\mathbb{D}(c_{ij} + c_{ji}) = \frac{1}{2}\mathbb{D}(c_{ij}) = \frac{1}{2}\mathbb{E}(c_{ij}^2) - \frac{1}{2}\mathbb{E}^2(c_{ij}) = \frac{1}{2}P\sigma_0^2.$$

From the semicircle law for random matrices (Lemma S3.1), the eigenvalues of $\boldsymbol{H} = \frac{1}{2}(\boldsymbol{C}^\top + \boldsymbol{C})$ are located in $\left[-r - \sqrt{2NP}\sigma_0, -r + \sqrt{2NP}\sigma_0\right]$ in a probabilistic sense as $N \to \infty$. Thus, to realize control requires $k > \eta_{\max} = \sqrt{2NP}\sigma_0 - r$ (**Condition-A**).

Mixed ecosystem. In a mixed network with competition and mutualistic interactions, we have $c_{ii} = -r$ and the off-diagonal elements (c_{ij}, c_{ji}) have the same sign, which with probability P are drawn from the distribution $(\pm|\mathcal{Y}|, \pm|\mathcal{Y}|)$ and are zero with probability $(1-P)$. We then have

$$\begin{aligned}
\mathbb{D}(\xi_{ij}) &= \frac{1}{4}\mathbb{D}(c_{ij} + c_{ji}) = \frac{1}{4}\left[\mathbb{D}(c_{ij}) + \mathbb{D}(c_{ji}) + 2\mathrm{Cov}(c_{ij}, c_{ji})\right] \\
&= \frac{1}{4}\left[2P\mathbb{D}(\mathcal{Y}) + 2\mathbb{E}(c_{ij}c_{ji}) - 2\mathbb{E}(c_{ij})\mathbb{E}(c_{ji})\right] \\
&= \frac{1}{2}\left[P\mathbb{D}(\mathcal{Y}) + \mathbb{E}(c_{ij}c_{ji})\right] = \frac{1}{2}P\left[\mathbb{D}(\mathcal{Y}) + \mathbb{E}^2(|\mathcal{Y}|)\right].
\end{aligned}$$

The semicircle law implies that the eigenvalues of $\frac{1}{2}(C^\top + C)$ are located in

$$\left[-r - \sqrt{2NP\left[\mathbb{D}(\mathcal{Y}) + \mathbb{E}^2(|\mathcal{Y}|)\right]}, -r + \sqrt{2NP\left[\mathbb{D}(\mathcal{Y}) + \mathbb{E}^2(|\mathcal{Y}|)\right]}\right]$$

in the probabilistic sense as $N \to \infty$. In particular, for $\mathcal{Y} \sim \mathcal{N}(0, \sigma_0^2)$, we have $\mathbb{D}(\mathcal{Y}) = \sigma_0^2$ and

$$\mathbb{E}(|\mathcal{Y}|) = \int_{-\infty}^{+\infty} |y|\frac{1}{\sqrt{2\pi}\sigma_0}e^{-\frac{y^2}{2\sigma_0^2}}\,dy = \sqrt{\frac{2}{\pi}}\sigma_0.$$

In this case, the eigenvalues of $\frac{1}{2}(C^\top + C)$ are located in

$$\left[-r - \sqrt{2NP\left(1 + \frac{2}{\pi}\right)}\sigma_0, -r + \sqrt{2NP\left(1 + \frac{2}{\pi}\right)}\sigma_0\right]$$

in the probabilistic sense as $N \to \infty$. Figure S2 shows the accuracy of the control criterion $k > k^* = \sqrt{2NP\left(1 + \frac{2}{\pi}\right)}\sigma_0 - r$ (**Condition-B**) obtained from the above estimated interval for the eigenvalue distributions. Figure S2 also shows how the growth of population size N affects the required control time and energy cost. These results agree well with the analytical estimates.

Predator-prey ecosystem. In this system, we have $c_{ii} = -r$ and the off-diagonal elements (c_{ij}, c_{ji}) have the opposite sign, which with probability P are drawn from the distribution $(\pm|\mathcal{Y}|, \mp|\mathcal{Y}|)$, and are zero with probability $(1-P)$. We have

$$\mathbb{D}(\xi_{ij}) = \frac{1}{2}\left[P\mathbb{D}(\mathcal{Y}) + \mathbb{E}(c_{ij}c_{ji})\right] = \frac{1}{2}P\left[\mathbb{D}(\mathcal{Y}) - \mathbb{E}^2(|\mathcal{Y}|)\right].$$

Applying the semicircle law, we have that the eigenvalues of $H = \frac{1}{2}(C^\top + C)$ are located in

$$\left[-r - \sqrt{2NP\left[\mathbb{D}(\mathcal{Y}) - \mathbb{E}^2(|\mathcal{Y}|)\right]}, -r + \sqrt{2NP\left[\mathbb{D}(\mathcal{Y}) - \mathbb{E}^2(|\mathcal{Y}|)\right]}\right]$$

in the probabilistic sense as $N \to \infty$. Especially, for $\mathcal{Y} \sim \mathcal{N}(0, \sigma_0^2)$, the eigenvalues of $H = \frac{1}{2}(C^\top + C)$ are located in

$$\left[-r - \sqrt{2NP\left(1 - \frac{2}{\pi}\right)}\sigma_0, -r + \sqrt{2NP\left(1 - \frac{2}{\pi}\right)}\sigma_0\right]$$

in the probabilistic sense as $N \to \infty$. The control criterion in the probabilistic sense becomes $k > \sqrt{2NP(1 - 2/\pi)}\sigma_0 - r$ (**Condition-C**).

IV. FLEXIBILITY OF CONTROL

We demonstrate the flexibility of control with different configurations of C and B_i using the ecosystems. In particular, the off-diagonal elements c_{ij} $(j \neq i)$ are constructed from an undirected scale-free network (SFN) [6] while the diagonal elements are chosen to be $c_{ii} = \xi - \sum_{j=1,j\neq i}^{N} c_{ij}$ with $\xi > 0$. We have $\lambda_{\max}(C) = \xi > 0$, so the uncontrolled system is unstable. With our controller $\boldsymbol{u}^S$, setting $k > \xi$ is sufficient for achieving control if we set $b_{ii} = 1$ for all i. In applications, it is desired to reduce the number of controlled nodes. We thus randomly select N_D nodes for control (i.e., $b_{i_j i_j} = 1$ for $1 \leq j \leq N_D$) and define $n_D \equiv N_D/N$.

We find that the energy cost decreases as n_D is increased (a result consistent with that in linear network control [7, 8]), as controlling more nodes can significantly reduce the control time, and increasing the mean degree m of the network can reduce both the control time and energy (for a given n_D value), as shown in Fig. S3(a). We also find that controlling high-degree nodes can reduce the time and energy for $n_D \lesssim 0.2$. However, if many nodes are accessible to control, controlling low-degree nodes can yield better performance, as shown in Fig. S3(b).

V. HINDMARSH-ROSE NEURONAL MODEL

We consider a small-world network of Hindmash-Rose (HR) neurons y_i with the coupling scheme $\sum_{j=1}^{N} c_{ij} \boldsymbol{\Gamma} h_{ij}(y_i, y_j)$, where $\boldsymbol{\Gamma} = \text{diag}[1, 0, 0]$ and $h_{ij}^S = u_i^S|_{x_i=y_j-y_i}$. In the network, the i-th neuron y_i $(1 \leq i \leq N)$ is described of the HR type [9]:

$$\begin{cases} \dot{y}_{i1} = y_{i2} - y_{i3} + 3y_{i1}^2 - y_{i1}^3 + I, \\ \dot{y}_{i2} = 1 - y_{i2} - 5y_{i1}^2, \\ \dot{y}_{i3} = -ry_{i3} + 4\nu(y_{i1} + 1.6), \end{cases}$$

where y_{i1} is the membrane potential, y_{i2} stands for the recovery variable associated with the fast current, y_{i3} is a slowly changing adaptation current, $I = 3.281$ is the external current input, and $\nu = 0.0012$ is the damping rate of the slow ion channel. Figure S4(a) shows that synchronization can be achieved rapidly through control. Comparing with the linear coupling scheme $h_{ij}^L = u_i^L|_{x_i=y_j-y_i}$, our controller h_{ij}^S leads to a faster transition, regardless of the network size N, as shown in Fig. S4(b).

---

[1] G. H. Hardy, J. E. Littlewood, G. Pólya, *Inequalities* (Cambridge University Press, Cambridge, 1988).

[2] W. Rudin, *Functional Analysis* (McGraw-Hill Science, Singapore, 1991).

[3] V. Lakshmikantham and S. Leela, *Differential and Integral Inequalities* (Academic Press, New York, 1969).

[4] E. P. Wigner, Ann. Math. **67** 325 (1958).

[5] G. W. Anderson, A. Guonnet, and O. Zeitouni, *An Introduction to Random Matrices* (Cambridge University Press, Cambridge, 2009)

[6] A.-L. Barabási and R. Albert, Science **286**, 509 (1999).

[7] Y.-Z. Chen and L.-Z. Wang and W.-X. Wang and Y.-C. Lai, Royal Soc. Open Sci. **3**, 160064 (2016).

[8] L.-Z. Wang and Y.-Z. Chen and W.-X. Wang and Y.-C. Lai, Sci. Rep. **7**, 40198 (2017).

[9] J. L. Hindmarsh and R. M. Rose, Nature **296** 162 (1982).
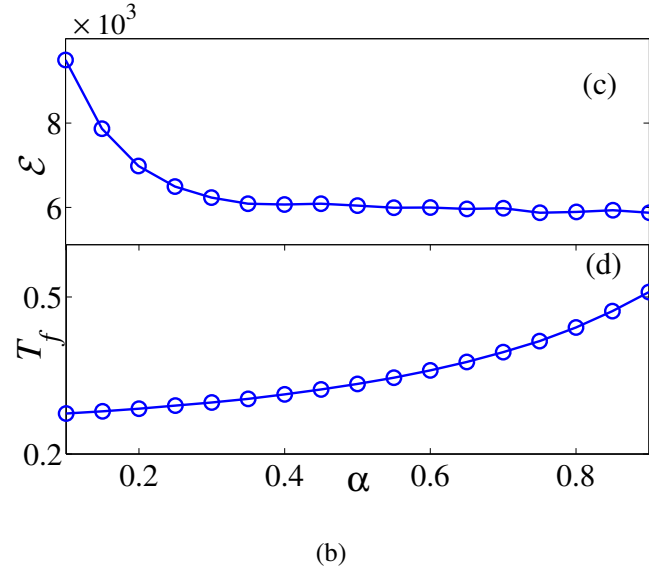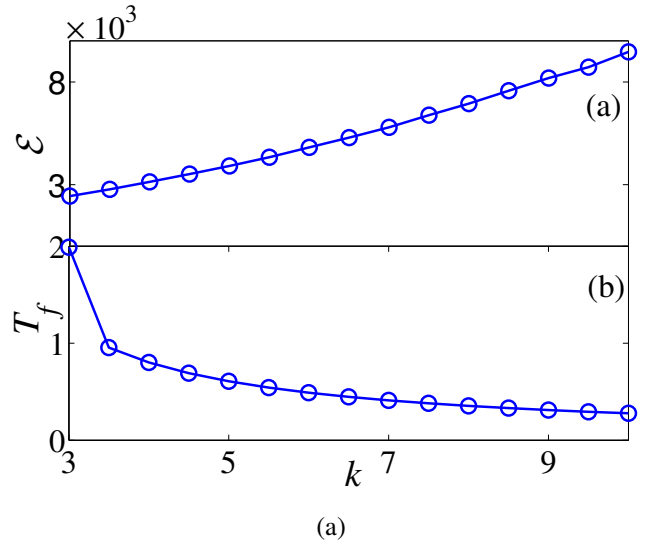
(a)

(b)

FIG. S1. **Trade-off between required control time and energy cost**. Effects of increasing k and α on control time and energy cost for the Florida food-web network: (a) energy cost versus k, (b) control time versus k, (c) energy cost versus α, and (d) control time versus α. The initial state values are randomly taken from the interval $[0, 5]$.
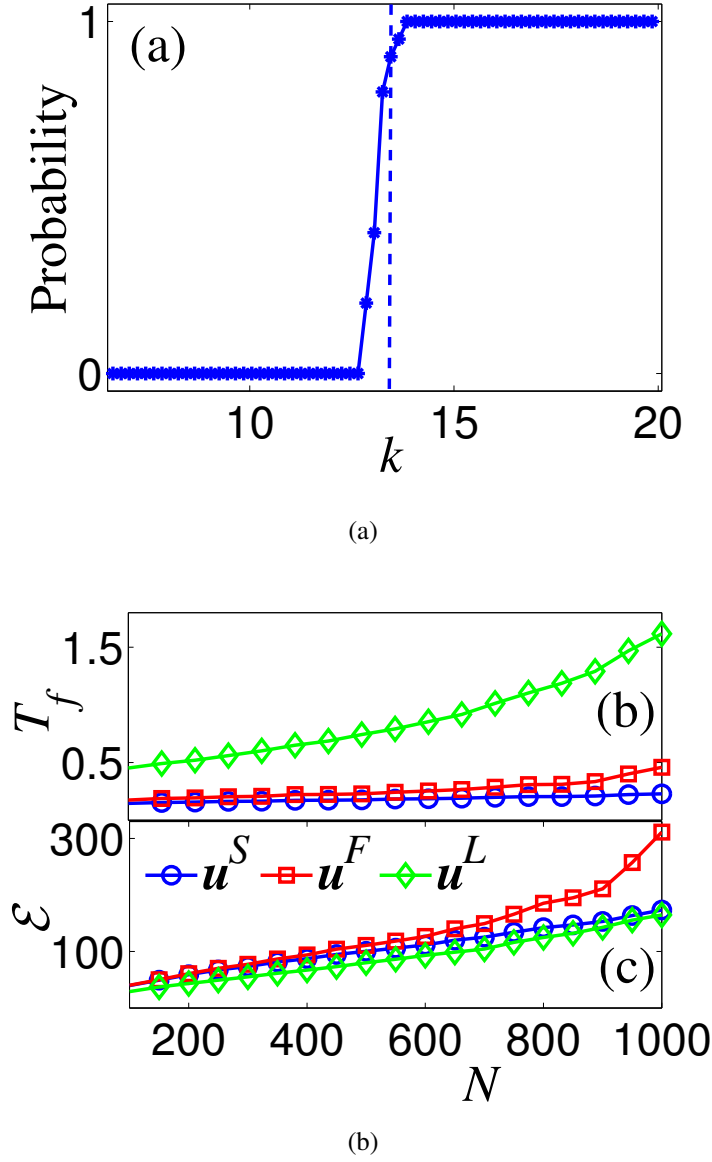
(a)

(b)

FIG. S2. **Eigenvalue distribution and estimates of the required control time and energy cost for mixed ecosystems**. (a) The probability of successfully controlling a mixed ecosystem when feedback control strength k passes through the critical value $k^* = \sqrt{2NP\left(1 + \frac{2}{\pi}\right)\sigma_0 - r}$ (indicated by the vertical dashed line). The probability is calculated by simulating 100 random matrices with $N = 250$, $P = 0.25$, $\sigma_0 = 1$, and $r = 1$. (b,c) Required control time and energy cost, respectively, for the controlled mixed ecosystem subject to controllers $\boldsymbol{u}^S$ (circles), $\boldsymbol{u}^F$ (squares) and $\boldsymbol{u}^L$ (diamonds). The parameters are $P = 0.25$, $\sigma_0 = 1$, $k = 1.1k^*$, $\alpha = 0.8$, and $N \in [50, 1000]$. All the initial state values of the networked system are randomly chosen from the interval $[-5, 5]$.
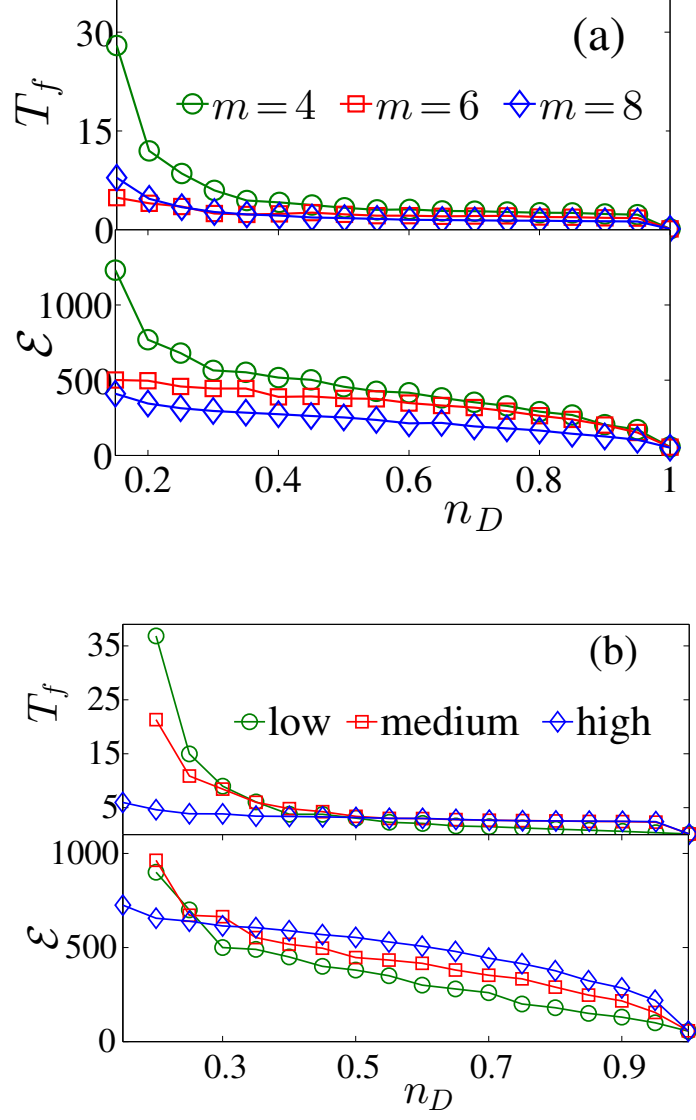
FIG. S3. **Flexibility performance with different control configurations**. For scale-free networks, control time and energy versus the density n_D of driver nodes for (a) mean degrees $m = 4,\ 6,\ 8$ and (b) $m = 6$ and driver nodes of high, medium, and low degrees. The network size is $N = 500$ and controller parameters are $\xi = 1$ and $k = 30$. Other parameters are the same as those in Fig. 4 in the main text.
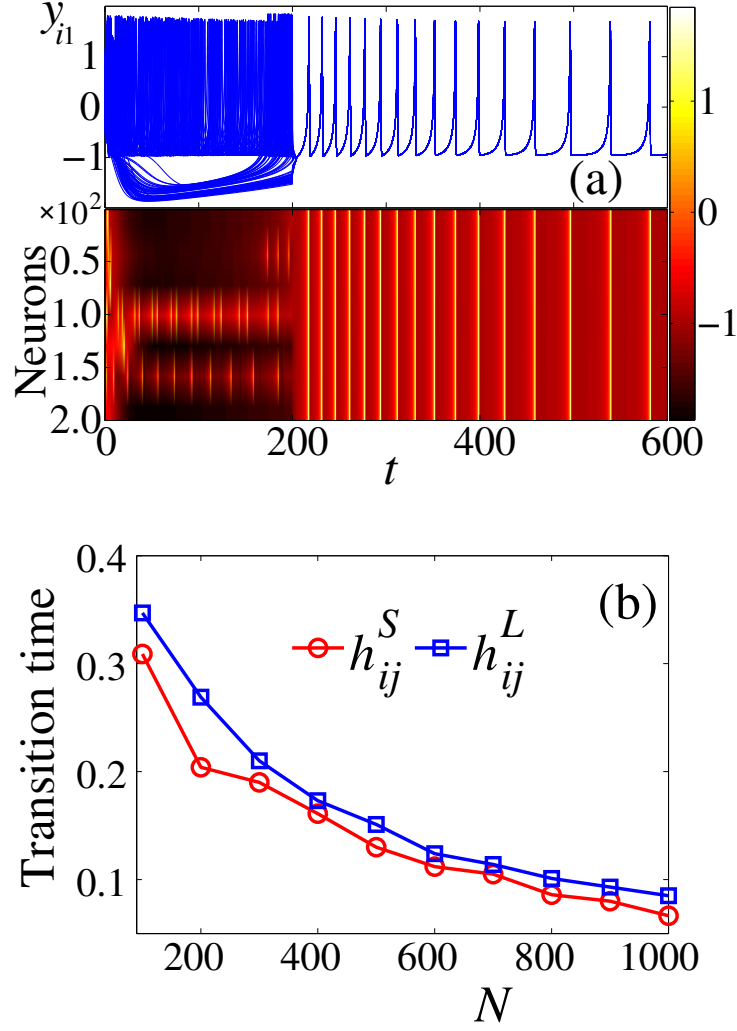
FIG. S4. **Controlled generation synchronization of spiking HR neuronal networks**. (a) Time course (upper) and color map (lower) of all potentials y_{i1} of a HR neuronal network, where $\alpha = 1/2$, $k = 0.15$, h_{ij}^S is activated at $t = 200$, and the rewiring probability 0.1 and $N = 200$ are used for generating the small-world network. (b) Synchronization transition time for different values of N.